Critical currents and pinning mechanisms in directionally solidified YBa$_2$Cu$_3$O$_7$-Y$_2$BaCuO$_5$ composites

B. Martínez, X. Obradors, A. Gou, V. Gomis, S. Piñol, and J. Fontcuberta
Instituto de Ciencia de Materiales de Barcelona, Consejo Superior de Investigaciones Científicas,
Campus Universitat Autònoma de Barcelona, Bellaterra 08193, Spain

H. Van Tol
High Magnetic Field Laboratory, 25 Avenue des Martyrs, Boîte Postale 166, F 38042 Grenoble Cedex 9, France
(Received 22 March 1995; revised manuscript received 2 October 1995)

The superconducting properties of directionally solidified YBa$_2$Cu$_3$O$_7$-Y$_2$BaCuO$_5$ composites, with critical currents above 10^5 A/cm^2 at 77 K and zero magnetic field, are reported in a wide variety of samples having very different contents of Y$_2$BaCuO$_5$ (211 phase) precipitates with different particle size and magnetic fields up to 22 T. The field, temperature, and composition dependence of the critical currents allow us to identify interfacial pinning by 211 precipitates as a very effective pinning mechanism. Nevertheless, single vortex interfacial pinning has a dominant role only in a narrow region below about 1 T and temperatures 40 K$\leq T \leq$80 K. In this region the system shows a behavior very akin to that observed in ion irradiated single crystals and described as correlated disorder. On lowering the temperature the thermal wandering of the vortex from secondary weak pinning centers decreases leading to a new single vortex pinning regime extending up to very high magnetic fields where a mixture of strong and weak pinning centers are active. On the other hand, increasing the magnetic field, the characteristic footprints of the small bundle and large bundle regimes are identified at intermediate temperatures. The former is found below the H-T line given by the maximum of the macroscopic pinning force while the latter is observed above this line up to the irreversibility line. Finally, collecting all these results together a magnetic phase diagram of the mixed state of the YBa$_2$Cu$_3$O$_7$-Y$_2$BaCuO$_5$ textured composites is proposed.

I. INTRODUCTION

One of the most promising fields for immediate application of the high-temperature superconductors is large scale power applications such as superconducting magnets, current leads, energy storage systems, etc. All these applications require a high current density flowing at tolerable low dissipation at 77 K. Unfortunately the ceramic character of these materials with its granularity and the appearance of weak links, which generally occur at grain boundaries due to grain misorientation[1] and chemical inhomogeneity at the interfaces,[2] have been serious problems to overcome. These problems have been solved by using various processing techniques such as melt texturing and thermomechanical methods.[3–5] Even though these techniques allow us to obtain good quality materials and to solve granularity problems, due to the high desirable operating temperature (77 K), the short coherence length, and the strong anisotropy of these materials, flux motion, which induces dissipation in the presence of transport currents, severely reduces the effective J_c that can be maintained in the presence of magnetic fields. Therefore, the improvement of the flux-pinning mechanism in the high-temperature superconductors is a subject of major interest.

It is well known that flux creep and flux pinning are extrinsic properties that depend on the interaction between the crystal defects and impurities and the flux lattice, then it is of great interest to examine the effects of different crystalline defects, such as twins boundaries, stacking faults, dislocations, etc. or nonsuperconducting inclusions on the flux-pinning capability of these materials. Even if the defect structure is well characterized it is not easy to find a direct correlation between the critical current J_c, and the actual microstructure of the samples. Such interaction between microstructure and flux lattice may be evaluated by using static pinning models which may give some predictions on the critical current density not influenced by thermally activated depinning. Nevertheless, in high-temperature superconductors thermally activated flux motion or flux creep is of considerable importance, thus preventing the correct determination of the unrelaxed J_c. The value of the measured current and its dependence on temperature and field are greatly influenced by thermal relaxation. There are some theoretical approximations that allow us to extract information from the measured critical currents by modeling relaxation. The standard analysis of magnetic relaxation due to thermal activation of vortex motion was proposed by Anderson and Kim[6] and assumes a linear dependence of the energy of the pinning barriers U, on the circulating currents. Other models with more complicated $U(J)$ relations, such as vortex glass[7] or collective-creep[8] models that predict a potential dependence of the energy of the pinning barriers on the current, have also been proposed to explain the experimental $J_c(T)$ dependencies. These models may help in order to get a more accurate description of the experimental data, that will allow us to ascertain which are the roles played by different potential candidates to effective flux-pinning centers in different regions of field and temperature.

The first step in order to improve flux pinning is the identification of the dominant pinning mechanisms, but this is not a trivial problem to solve in such a complicated system as the

123/211 ceramic composites in which the defects of the crystal structure and the nonsuperconducting precipitates of 211 phase coexist. Many efforts have been devoted to determine the role played by twin planes,[9,10] dislocations,[11,12] stacking faults,[13] oxygen deficiencies,[14] 211 precipitates,[15] and irradiation-induced defects[16–18] in providing effective pinning for the flux lines. The idea that 211 inclusions, with sizes that are about two orders of magnitude bigger than the coherence length, may act as an effective pinning center has been long put under question. Nevertheless, some experimental results obtained in 123/211 composites indicate that J_c at 77 K scales with the effective 123/211 interface area,[15,19,20] results that have been also confirmed in our own samples.[21] Whether the pinning is provided by the 123/211 interface itself, where the free-energy gradient is maximum, or by structural defects associated with it is still an open question.

In this work we report a careful study of the dependence of the critical currents on field and temperature in a wide variety of samples, having very different content of 211 phase precipitates of different size, in order to identify the dominant pinning mechanism in the different field regions and then design a procedure to increase the critical currents.

The paper is organized as follows: First, the temperature dependence of the critical currents at different fields is addressed. The results are analyzed from the scope of the vortex glass[7] and the collective-pinning–collective-creep theories[8] and similarities with other systems with quenched disorder, such as irradiation-induced columnar defects[22] with correlated disorder,[23] are also considered. The field dependence of the critical currents is considered next. Firstly the low-field region is studied and the different pinning regimes are analyzed on lowering temperature. Then, we have studied the high-field region identifying different pinning regimes through the field dependence of the critical current and results have been compared with those obtained in other $YBa_2Cu_3O_7$ samples.[24] We have also performed a complete study of the scaling of the macroscopic pinning forces. A complete study of the field and temperature dependences of the critical currents in the $H \| ab$ geometry will be reported elsewhere in the next future. Finally, collecting all the results from the thermal and field dependence of J_c a magnetic phase diagram of the mixed state of the 123/211 composites is proposed together with several suggestions concerning different possibilities of improving the critical currents.

II. EXPERIMENTAL

The samples used in this work have been fabricated by using a directional solidification method based in a vertical Bridgman technique that allows us to obtain quasi-single-crystalline superconducting bars (up to 12 cm in length and 1 cm^2 of cross section) with a fine distribution of precipitates of Y_2BaCuO_5 (211 phase).[5] A complete characterization of the microstructure of these samples by using transmission electron microscopy (TEM) may be found elsewhere.[25] For comparison purposes we have also used in some cases $YBa_2Cu_3O_7$ single crystals which were grown by the self-flux method in a gold crucible and oxygenated during five days at 450 °C.

The magnetic characterization of the samples has been carried out by using a superconducting quantum interference device magnetometer up to 5.5 T and extraction magnetometry at Service National des Champs Magnetiques Intenses (Grenoble) up to 22 T. The samples used for magnetic measurements have been cut from the bars and have a long dimension along the magnetic-field direction and one of the transversal dimensions small enough to have a small full penetration field H^* in order to minimize the self-field effects. Typically samples are parallelepipeds in shape with about $2.5 \times 1.5 \times 0.4$ mm^3 of volume. Special care must be taken in this point since it is expected that the role played by the 211 inclusions as effective pinning centers should be dominant in the low-field region. Thus, reliable experimental data points are needed in the low-field range to make it possible to derive some conclusions about flux-pinning mechanisms in this field region.

The inductive critical currents were obtained from the irreversible magnetization of the hysteresis loops by using the anisotropic Bean model in which $J_c^{ab} \approx 20 \Delta M / [a(1 - a/3b)]$, being $a \le b$ the sides limiting the surface perpendicular to the applied field and ΔM the difference between the upper and the lower branches of the hysteresis loops.[26]

The actual content of the 211 phase in the samples was determined by measuring the paramagnetic susceptibility and fitting a Curie-Weiss law in the high-temperature region ($T \ge 120$ K). The 211 phase percentage may be obtained through the relation $(\mu_{exp}/\mu_{211})^2 \times 100$, where μ_{exp} is the experimental magnetic moment obtained from the Curie-Weiss law and μ_{211} is the magnetic moment of the 211 pure phase. The distribution of sizes of the 211 phase precipitates has been deduced by means of image analysis of scanning electron microscopy pictures obtained in all the samples used in this work.[27] The mean size of the 211 particles of the different samples are comprised between 0.5 and 2 μm.

The actual content of 211 phase in the samples ranges from 4% to approximately 38% in volume. Some of the samples, those having the higher concentrations of 211 phase, do also have a small amount of CeO_2 (below 1% by weight). The benefits of such addition have been already reported[28] and, for the purpose of the present work, may be summarized as a means of refinement of the mean size of the 211 precipitates. This is a consequence of the modification of the growth mechanism and the increase of the processing temperature.

After the directional solidification process superconducting bars are oxygen deficient, thus an oxygenation treatment is needed after the texturation process. This treatment has been carried out at 450 °C under oxygen atmosphere and carefully monitored by using ac susceptibility measurements, since we have observed that it plays a major role in the final superconducting performances of the samples. We have recently analyzed in detail the relevance of the oxygenation process in the microstructure and critical currents of melt-textured 123/211 ceramic composites[14,29] and we will just summarize the main conclusions here for completeness.

In samples with deficient oxygenation[14] optical microscopy shows a layeredlike structure in which bands, parallel to the *ab* planes, of fully and partially oxygenated materials coexist. This structure may be easily identified through the zero-field-cooled (ZFC) susceptibility, with the applied field
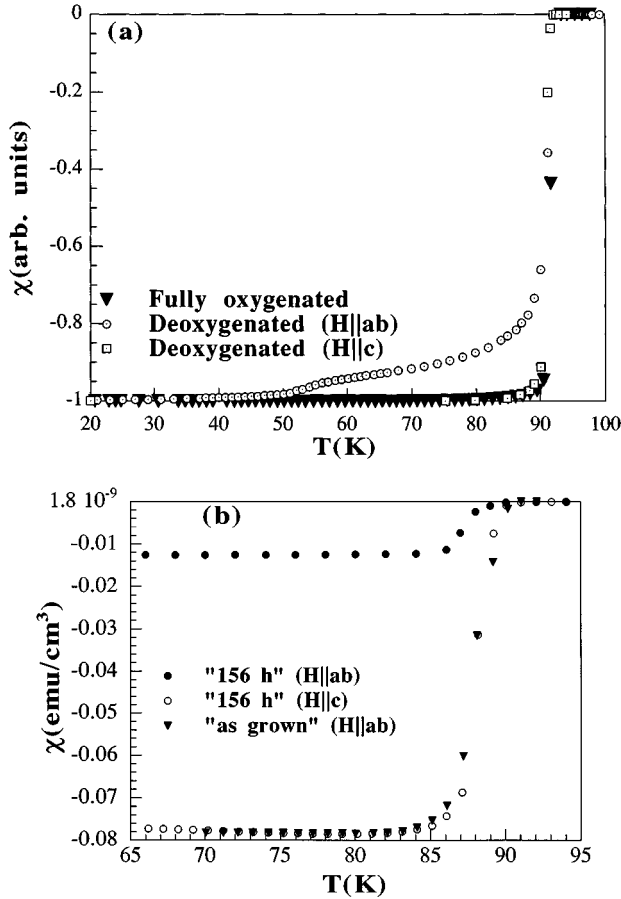
FIG. 1. (a) ZFC magnetic susceptibility of partially oxygenated ($H\|ab$ and $H\|c$) and fully oxygenated ($H\|c$) sample ($H=10$ Oe). (b) ZFC dc susceptibility showing the dependence of the shielding capability on the orientation of the applied field and the degree of aging.

parallel to the ab planes, that shows how parts of the sample, poorly oxygenated, progressively become nonsuperconducting as temperature is increased. As a result of this layered oxygen deficiency a considerable decrease of the critical currents is observed in both field orientations $H\|ab$ and $H\|c$.

Nevertheless, we have also observed that a long lasting oxygenation process may also be detrimental for the final superconducting performances of the samples giving place to aging processes.[11] The chemical decomposition of $YBa_2Cu_3O_7$ in areas surrounding microcracks, that are the channels through which oxygenation preferentially takes place, together with an enormous increase of stacking faults and dislocations have been identified by means of TEM in aged samples, leading to a notorious decrease of the critical currents and a strong shift of the irreversibility line.

In order to avoid these problems we have carefully monitored the oxygenation process by using low-field dc and ac susceptibility with the external field applied parallel to the ab plane. In oxygen-deficient samples, the zero-field-cooled susceptibility easily allows the identification of poorly oxygenated bands through the changes in the magnetic shielding capability [see Fig. 1(a)].

It is very important to stress that the optimization of the oxygenation process is very dependent on the actual micro-

structure of the samples since oxygen diffusion takes place mainly through the microcracks, whose size, length, and density is severely affected by the 211 phase content of the samples, thus making it difficult to know "*a priori*" which is the optimum oxygenation time for each sample. This is probably the main problem when a complete analysis of the pinning mechanisms in 123/211 composites is being carried out. We would like to point out that all the experimental results reported in this paper have been obtained in samples where the oxygenation process has been optimized independently. However, we note that the more stringent effects associated to the oxygenation process occurs at high magnetic fields.[29]

Regarding the role played by microcracks on the critical currents, we would like to emphasize that all the results presented in this paper have been obtained in the $H\|c$ geometry and microcracks are not likely to affect pinning in this geometry. Nevertheless, we have already done a careful microstructural characterization of the samples, in which the problem of microcracks is addressed (see Sandiumenge *et al.*[29]).

III. EXPERIMENTAL RESULTS

A. Temperature dependence of the critical currents

We have studied the thermal dependence of the critical currents in a series of samples having different content of 211 phase ranging from 4% to approximately 38%, once we have checked that samples have been correctly oxygenated but avoiding aging effects. Samples were cooled in a maximum field of 5.5 T down to 5 K then the field is lowered to the desired value and the magnetization measured as temperature is increased up to 92 K. A brief summary of these measurements has been previously reported.[30] It is important to stress that we have indeed verified, by measuring at different waiting times up to 15 min, that the main features of the $J_c(T)$ curve are unchanged by flux-creep effects except at very high temperatures approaching the irreversibility line. This point will be addressed later in connection with the proposed magnetic phase diagram.

We should also note that this experimental procedure, when performed in zero external applied field, leads actually to a $J_c(T)$ curve measured under the trapping field H_t. However, because of the geometry of the samples, the trapped field turns out to be in all the cases smaller than about 4 kOe. In this way, the temperature dependence of $H_t(T)$ have a very small influence on the experimental $J_c(T)$ curves obtained in zero external field.

In Fig. 2(a) we show the thermal dependence of J_c^{ab} ($H\|c$) in self-field for several textured samples having different contents of 211 precipitates and a single crystal. First of all, it is worth mentioning that a net increase of the critical currents with the increase of the 211 precipitates is clearly observed and what is even more important: the thermal dependence of the critical current in the single crystal is much higher than in the textured samples. This difference is better appreciated in Fig. 2(b) where we plot the normalized critical currents of the different samples and the single crystal. An important point to note also is that the temperature dependence of J_c^{ab} is softened above 40–50 K leading to a maximum enhancement around 70–77 K where values above 10^5 A/cm^2 are obtained. Then, our results make evident that some fundamental difference exists between the pinning
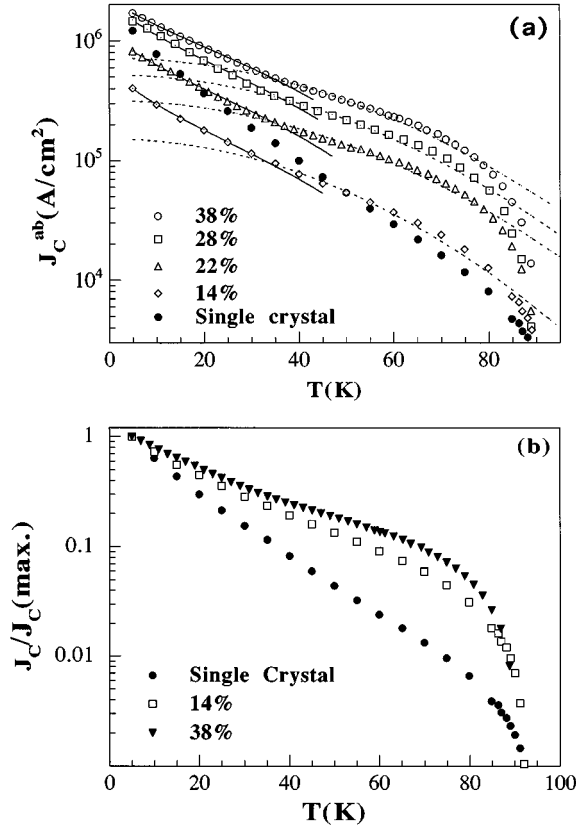
FIG. 2. Temperature dependence of J_c^{ab} in a single crystal and textured ceramic samples with different content of 211 phase in self-field. (a) Solid lines correspond to the fitting by using Eq. (2), while dashed lines correspond to the fitting by using Eq. (5) in the text. (b) Normalized $J_c^{ab}(T)$ curves showing the effect of the 211 inclusions.

mechanism in the single crystal and in the textured samples which leads to a stronger temperature dependence of the critical currents in the former. This effect is probably a consequence of the existing 211 precipitates which also induce the observed softening of $J_c^{ab}(T)$ at intermediate temperatures.

For the time being we will examine if the observed temperature dependence of J_c may be interpreted in the light of the existing theoretical models. As we have already mentioned, magnetic relaxation in high-temperature superconductors is very large and dominates the temperature dependence of J_c. All the flux-creep theories share the same basic idea that magnetic relaxation is originated on the thermal activation of the flux lines over an effective energy barrier U,[6] and that this leads to a reduction of the apparent critical currents.

The simplest model, introduced by Anderson and Kim,[6] assumes a linear relation between the energy of the barriers U, and the circulating currents, $U(J) = U_0[1 - (J/J_{c0})]$. Where U_0 and J_{c0} are, respectively, the temperature-dependent energy barrier and the critical current density in absence of flux creep. This relation leads to the well-known flux-creep relation

$$J_c(T) = J_{c0}\left[1 - \left(\frac{T}{U_0}\right)\ln\left(\frac{t}{t_{\text{eff}}}\right)\right], \qquad (1)$$

where t_{eff} is an effective attempt time. Then, the temperature and time dependences of J_c are contained in two factors, J_{c0} whose temperature dependence is BCS like, and the factor in brackets that accounts for the flux-creep effects.

More sophisticated models of relaxation have been developed that include the possibility of a nonlinear relationship between U and J in order to reproduce the observed experimental data.[7,8,31,32] In this sense, a logarithmic dependence of the form $U(J) = U_0\ln(J_{c0}/J)$ was proposed by Zeldov *et al.*[32] leading to a potential relation for $J_c(T)$. The vortex glass[7] and collective-pinning–collective-creep[8] theories lead to an inverse power-law form for $U(J)$ namely, $U(J) = (U_0/\mu)[(J_{c0}/J)^{\mu} - 1]$ with a characteristic exponent μ. In these later theories the temperature dependence of U is implicit in the quantities U_0 and J_{c0}.

From this inverse power-law form of $U(J)$, the following expression is obtained for $J_c(T)$:

$$J_c(T) = \frac{J_{c0}}{\left[1 + (\mu T/U_0)\ln(t/t_{\text{eff}})\right]^{1/\mu}}. \qquad (2)$$

In order to evaluate the temperature dependence of our experimental $J_c(T)$ we will follow a procedure similar to that described in Ref. 33 for single crystals of $YBa_2Cu_3O_7$ and will assume that J_{c0} and U_0, whose temperature dependence is not known *a priori*, vary with temperature in the following form:

$$J_{c0}(T) = J_{c00}\left[1 - \left(\frac{T}{T_c}\right)^2\right]^n, \qquad (3)$$

$$U_0(T) = U_{00}\left[1 - \left(\frac{T}{T_c}\right)^2\right]^n. \qquad (4)$$

These simple phenomenological laws are derived from the BCS temperature dependence of the coherence length and the thermodynamical critical field. In order to minimize the number of fitting parameters and, since our main interest is the composition dependence of the most relevant parameters, we have fixed some of them to some reasonable values, namely $\ln(t/t_{\text{eff}}) \approx 33$ and $n = 3/2$. In choosing these values we have made use of the data given in Ref. 33 for $YBa_2Cu_3O_7$ single crystals and the same considerations in choosing the parameter $n = 3/2$ for both $J_{c0}(T)$ and $U_0(T)$ are valid here. Regarding the value of the exponent μ we have taken $\mu = 1/7$ that is the predicted value for the case of single vortex pinning by weak pinning centers in the framework of the vortex glass theory.[7,8] So finally the unique fitting parameters are the nonrelaxed critical current J_{c00}, and the energy of the pinning barrier at $T = 0$ K, U_{00}. The result of the fitting to the experimental data by using Eq. (2) is shown in Fig. 2(a), good fits are obtained for all the samples for temperatures below about 40 K, while a systematic softening of the temperature dependence is observed between 40 and 80 K which cannot be described by this model. Then, our results show that, in the region of low fields, the low-temperature ($T \leq 40$ K) dependence of $J_c(T)$ is consistent with the single vortex behavior predicted by the vortex glass–collective-pinning theory.
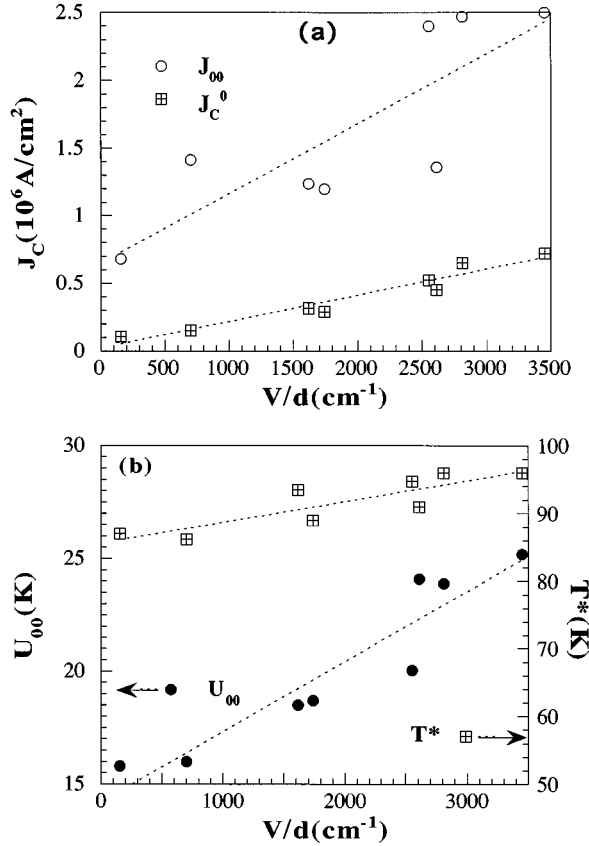
FIG. 3. (a) Dependence of the nonrelaxed critical current J_{c00} and J_c^0, obtained from the fittings by using Eqs. (2) and (5), respectively, on the 123-211 interface specific area in the $H\|c$ geometry and in self-field conditions. (b) Dependence of the pinning energy U_{00} and T^* on the 123-211 interface specific area in the same conditions as above.

At higher temperatures, in the temperature range (40 K$\leq T \leq$80 K), we have found that $J_c(T)$ may be properly described by the following expression:

$$J_c(T) = J_c^0 \exp[-3(T/T^*)^2], \qquad (5)$$

as it is also shown in Fig. 2(a) (dashed line). This expression has been proposed to account for the temperature dependence of the critical current in the case of linear correlated disorder[23] and has been experimentally observed in $Bi_2Sr_2CaCu_2O_8$ single crystals having columnar defects generated by ion irradiation.[22] The 123/211 interfaces may actually be considered also as a source of correlated disorder where strong pinning occurs. Similarities and differences will be analyzed later on.

In Figs. 3(a) and 3(b) we show the evolution of the fitting parameters obtained by using Eqs. (2) and (5), J_{c00} and J_c^0 and U_{00} and T^*, respectively, as a function of the composition of the samples represented by the parameter V/d. We have chosen the quantity V/d, i.e., the ratio of the volume percentage of 211 phase precipitates and their mean diameter, because this parameter is a measure of the interface area between 211 particles and 123 superconducting matrix and therefore, may shed some light on the role played by the interfacial pinning mechanism in the pinning processes of our samples.
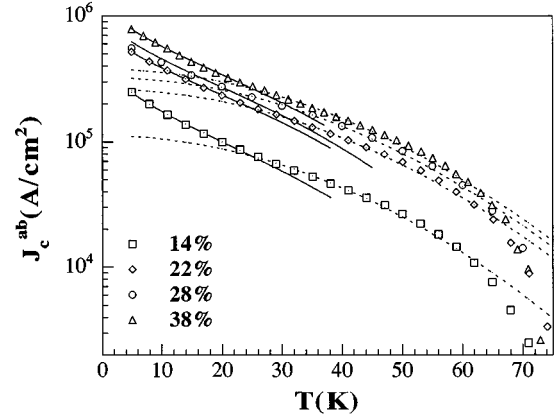

FIG. 4. Temperature dependence of J_c^{ab} in a single crystal and textured ceramic samples with different content of 211 phase in a field of 3 T ($H\|c$). Solid lines correspond to the fitting by using Eq. (2) and dashed lines correspond to the fitting by using Eq. (5) in the text.

In both Figs. 3(a) and 3(b), we observe that a linear relation does exist between the four parameters, J_{c00}, U_{00}, J_c^0, and T^*, and V/d giving strong indications that interfacial pinning is indeed active in these materials. However, it is worth mentioning here that the parameters J_c^0 and T^*, determined in the high-temperature regime (40 K$\leq T \leq$80 K), do show a linear dependence on V/d, while J_{c00} and U_{00} are much more scattered, thus suggesting that 123/211 interfacial pinning is the dominant pinning mechanism in this high-temperature–low-field region of the magnetic phase diagram, while at low temperatures additional pinning centers may become active. Our results are then a nice verification and clarification of the interfacial pinning mechanism proposed by Murakami et al. from their measurements at 77 K.[19] We show that the linear relationship previously observed between J_c and V/d at T=77 K and H=1 T (Ref. 19) arises mainly from an increase of the T=0 K pinning force (J_c^0 or J_{00}), while the decrease of the thermal activation effects only accounts for a small percentage of the change observed in J_c^{ab} since the observed variation of U_{00} and T^* is moderate. It should also be mentioned that the values we obtain for the pinning energy are quite similar to those reported for proton-irradiated $YBa_2Cu_3O_7$ single crystals.[33]

Another interesting feature to note is that the temperature dependence of the measured critical current of a $YBa_2Cu_3O_7$ single crystal is much stronger than in the 123/211 ceramic composites [see Fig. 2(b)]. This fact indicates essentially that the activation energy U_0, in Eq. (3) is smaller in the single crystal than in our textured samples, thus giving further support to our conclusions concerning the effectiveness of the 211 precipitates as active pinning centers in the low-field regime, since these pinning centers are absent in the single crystal. The differences between the single crystal and 123/211 composites become more evident in the high-temperature regime (40 K$\leq T \leq$80 K), i.e., where 123/211 interfacial pinning plays the dominant role.

Finally, we would like to mention that we have also studied the temperature dependence of the critical currents obtained at H=3 T (see Fig. 4). It is worth signaling that the differences observed in the critical currents at low fields for
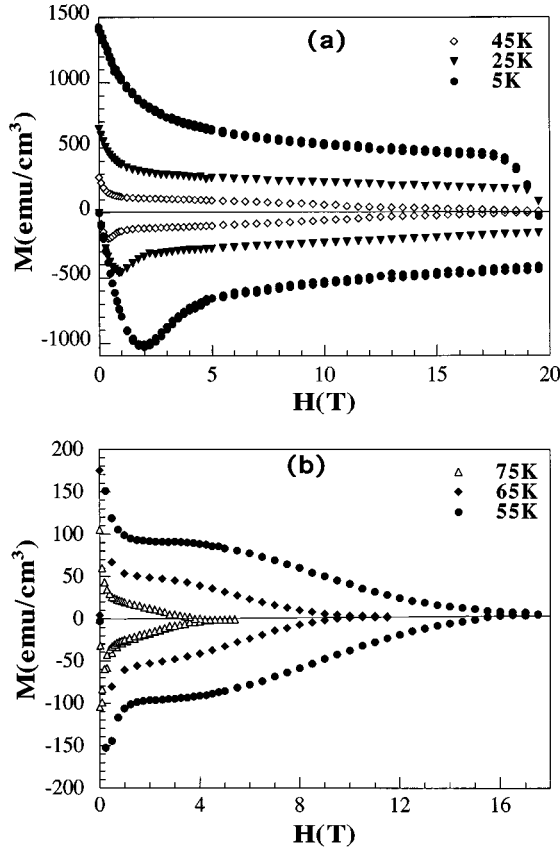
FIG. 5. Magnetization loops of the sample having 38% of 211 phase and 1% of CeO$_2$ for several temperatures with the applied field parallel to the c axis.

FIG. 6. (a) and (b). Field dependence of the inductive critical currents derived from the hysteresis loops with $H \| c$ for several temperatures for the sample with 38% of 211 phase and 1% of CeO$_2$.

samples having different 211 phase contents have clearly diminished and even the single crystal, with no 211 phase at all, has very similar values. This fact clearly suggests that different pinning mechanisms are active at low fields ($H \leqslant 1$ T) and high fields. With this field of 3 T the fitting by using Eq. (2) can also be carried out by using the same values of n and μ but the dependence of the different parameters on V/d are much more scattered. Equation (5) also may be used above about 30 K but, as in the case of Eq. (2), the fitting parameters have a scattered behavior when depicted vs V/d. Therefore, to derive reliable conclusions about the pinning mechanisms in this high-field region is not a simple task. The reasons for this complex behavior will become more apparent later on in connection with the proposed H-T magnetic phase diagram for the 123-211 superconducting composites.

B. Magnetic-field dependence of the critical currents

Typical hysteresis loops of our samples with the external applied field parallel to the c axis are shown in Fig. 5 for several temperatures. None of the samples used in this work do show signals of the fishtail effect, but its features have been observed in some aged samples.[29] Critical currents of the sample having 38% of final content of 211 phase ($V/d \approx 3450$ cm^{-1}) and 1% of CeO$_2$ are shown in Figs. 6(a) and 6(b) for several temperatures, with the external applied field parallel to the c axis.

From the visual observation of the hysteresis loops at low and intermediate temperatures it becomes immediately clear
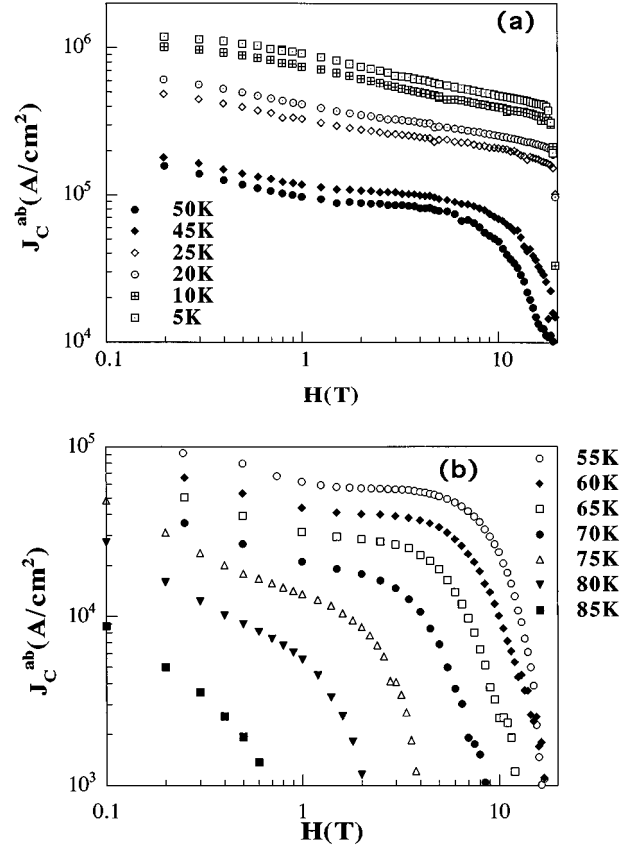
that the field dependence of the irreversible magnetization strongly differs in different regions of the H-T phase diagram suggesting that different pinning mechanisms play the dominant role in each region. It seems reasonable to expect that at least three different pinning regions exist, one at low fields up to 1–2 T, another one above 2 T, characterized by a weak field dependence of the critical currents, and finally a third one with a fast decrease of J_c up to the irreversibility line. In the low-field region the vortex lattice parameter $a_f = 1.075(\Phi_0/B)^{1/2}$ is large, then vortex are almost independent and single vortex pinning may be expected. For example for $H = 1$ T the vortex lattice parameter is $a_f \approx 450$ Å which is well below the dimensions of the interparticle separation of the 211 precipitates in the samples. This suggests that below this magnetic field more than one vortex may become trapped at the interface of the 211 particles if they are soft enough to bend and accommodate to the random distribution of the 211 particles. Then, we expect that in the low-field region the interfacial pinning by the 211 precipitates will be the dominant pinning mechanism and the random distribution of small precipitates will induce an important bending of the vortex to take advantage of the strong pinning associated to 123/211 interfaces. However, there must be a crossover to a different pinning mechanism in the high-field regime. This scenario does change on lowering temperature as new pinning centers become active. Those new active pinning centers (twin planes, oxygen defects, dis-

locations or whatever) contribute to pin the vortex stronger and the field dependence of the critical current decreases, at the same time the dominant role played by the 211-123 interfacial pinning fades away among the contributions from the rest of the pinning centers. In this sense, the change observed in the thermal dependence of the critical currents around 40 K is naturally identified as a depinning temperature at which thermal fluctuations overcome the energy of the pinning barriers of some pinning centers that become inactive and only the strongest, i.e., 123-211 interfacial pinning mainly, remains active up to higher temperatures. We will proceed now to analyze the different field region mentioned above.

1. Low-field regime

In this section we will try to confirm, from the analysis of the field dependence of the critical currents, the results obtained from the thermal behavior of the critical currents indicating that, in this field region, interfacial pinning by 123/211 interfaces are the dominant pinning mechanism.

There has been a controversial issue regarding the question to what extent these nonsuperconducting particles may represent an effective vortex pinning center since their sizes ($\approx 0.1–1$ μm) are very large compared with the coherence length of the high-T_c superconductors ($\xi_c \approx 3$ Å and $\xi_{ab} \approx 15$ Å for YBa$_2$Cu$_3$O$_7$). The question was addressed by Murakami and co-workers[15,19,20] in the framework of single vortex pinning model based on the core condensation energy. In the case of a large pinning center the depth of the pinning potential U_p, is large, but the pinning force is given by the gradient and this is maximum at the interfaces. Therefore vortex are mainly pinned at the interface between normal and superconducting regions. Then, an important point in order to have an effective interfacial pinning is to have clean 123/211 interfaces free from secondary phases, amorphization, etc. to assure a strong gradient of the order parameter.

In the single vortex pinning regime, the flux lines will bend in order to become pinned at the 211-123 interfaces, and a simple summation of the individual microscopic pinning forces may be performed leading to[15,19]

$$J_c^{ab} = \frac{\pi \xi_{ab} B_c^2 N_p d^2}{4 \mu_0 \phi_0^{1/2} B^{1/2}} \approx \beta B^{-1/2}, \quad (6)$$

where N_p is the number of 211 inclusions per unit volume and d is their mean size. Thus, J_c is proportional to $N_p d^2$, which corresponds to the quantity V/d, being $V \approx N_p d^3$ the volume fraction of the 211 precipitates. In order to check the occurrence of the interfacial pinning mechanism in our samples we have fitted our experimental $J_c(H)$ curves by using Eq. (6) obtaining a very good agreement in the range of fields below 1.5 T and temperatures above 45 K. An example of the results obtained is shown in Fig. 7. As we will discuss later, the field where the law represented by Eq. (6) changes corresponds to a crossover field to a new pinning regime. If the hypothesis of interfacial pinning is correct the parameter β in Eq. (6) should display a linear dependence on V/d as it is, in fact, observed for several temperatures (see Fig. 8). A preliminary report of these results has already been presented (21). Nevertheless, it should be mentioned that on lowering temperature a progressive departure from the above
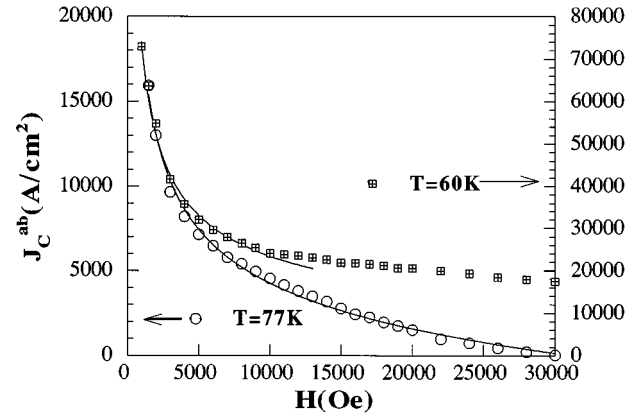

FIG. 7. Field dependence of the critical currents at $T=60$ and 77 K. The lines correspond to the fit of the experimental data by using Eq. (6) in the text.

simple picture, i.e., $J_c \propto B^{-1/2}$, is observed even in the low-field region. This behavior is clearly evident in Fig. 9, where we show a log-log plot of J_c vs H showing up the validity of a power-law dependence, i.e., $J_c \propto B^{-\alpha}$ over a broad temperature range. However, it is evident from the picture that the value of α changes when different regions of fields are considered and also changes with temperature for a given region of fields. In the high-temperature range the value of α is 1/2 in the low-field region, i.e., $H \leq 1.2$ T approximately, while with increasing field (H above 2 T approximately) a "plateau" in which J_c is almost field independent, $\alpha \approx 0.1$, develops before the irreversibility line is approached. The plateau zone becomes more evident as temperature decreases but it has almost disappeared above about 65–70 K approximately. For intermediate temperatures, 50 K$\geq T \geq$ 20 K, the value of α in the low-field region slowly decreases from 0.5 to 0.3, while that of the plateau zone increases from 0.1 approaching 0.3. Below about 15 K a unique value $\alpha \approx 0.3$ describes the field dependence of J_c in all the ranges of field up to 22 T.

2. High-field regime

After a fast decrease of the irreversible magnetization $M(H)$, or the critical currents $J_c^{ab}(H)$ in which $\alpha \approx 1/2$, a
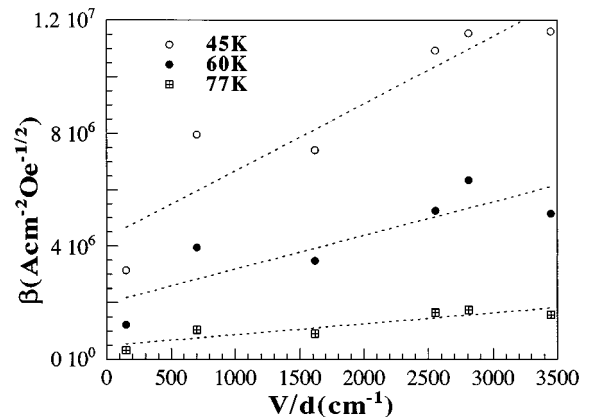

FIG. 8. Composition dependence of the parameter β in Eq. (6) for several temperatures.
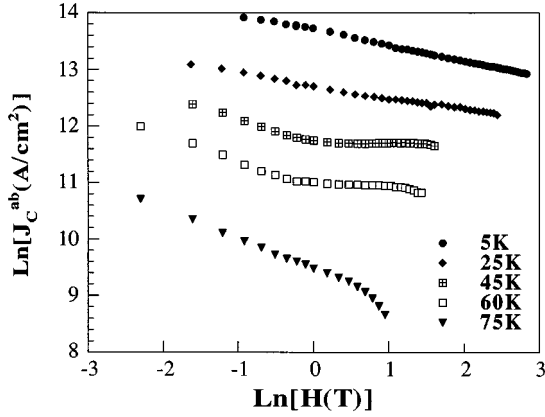
FIG. 9. Log-log plot of J_c vs H making evident the existence of a power-law dependence between them, i.e., $J_c \approx H^{-\alpha}$. The value of α clearly changes from $\alpha = 1/2$ in the high-temperature and low-field regime to $\alpha = 0.3$ in the low-temperature regime and in a very broad range of fields (up to the maximum field measured about 22 T). A crossover is observed between both values at intermediate temperatures.

regimen in which the field dependence of $M(H)$, or $J_c^{ab}(H)$, is very smooth ($\alpha \approx 0.1$) is reached in a wide region of fields above 1.5–2 T (Figs. 7 and 8). On lowering the temperature the values of the α exponent in the low- and high-field regions slowly approach each other and below about 20 K all the $J_c(H)$ curves may be described with only one value of $\alpha \approx 0.3$. The crossover field between these two regions depends on temperature but stabilizes around 1.5–2 T at high temperature. Above 1.5–2 T we observe that J_c is almost independent of the parameter V/d, thus indicating that interfacial pinning only plays a secondary role in the high-field region.

Finally approaching the irreversibility line (IL) a much faster decrease of the critical currents is observed. In this part of the $J_c(H)$ curves it is possible to identify, for some temperatures, a region in which $J_c \propto H^{-3}$ before reaching the irreversibility line (see Fig. 10). This law is clearly identified in the temperature region where the "plateau" in $J_c(H)$ is well separated from the irreversibility line and the maximum magnetic field available is high enough to reach this line. In
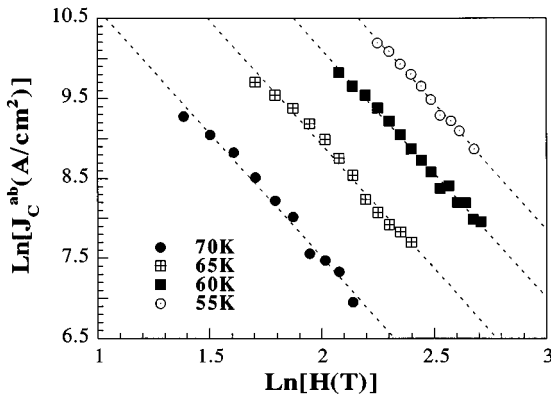
our experimental data this zone is restricted between 70 and 50 K. This field dependence of the critical current has been theoretically predicted for the so-called large bundle regime[23] in the collective-pinning theory and indeed, experimentally observed in YBa$_2$Cu$_3$O$_7$ single crystals.[34]

In order to get some information about the relevant pinning mechanism it is customary to look for the scaling of the volume pinning force $F_P(B,T) = BJ_c(B,T)$. Usually all the quantities determining F_P can be written in terms of the internal field B, and the temperature-dependent critical fields of the superconductor which in the cases where thermal activation effects are negligible lead to the following general form for F_P :[35,36]

$$F_P(b,T) = F_{P0}(T)b^p(1-b)^q \tag{7}$$

where the exponents p and q are characteristic of the active pinning mechanism and $b = B/H_{c2}$ is the reduced field, being H_{c2} the upper critical field. Then, all the $F_P(B,T)$ curves measured at different temperatures can be superimposed in a single curve of $F_P/F_{P\ max}$ vs b provided that the dominant pinning mechanism is the same in all the temperatures and fields considered. The absence of scaling can also give some information about the flux-pinning processes since some kind of structural feature, such as geometric matching effects or thermally activated flux motion should destroy the scaling behavior. Nevertheless, it should be mentioned that in the above model the structure and the elasticity of the flux-line lattice (FLL) are not taken into consideration.

A different approach to the problem was given by Kramer[37] developing a model which takes explicitly into account the properties of the flux-line lattice. In this model exponents of $p = 1/2$ and $q = 2$ are predicted and the decrease of F_P to zero at high fields is due to the reduction of the shear modulus of the lattice. At $F_P = 0$ the lattice has completely melted and this occurs at a field $H^*(T)$, that may be different from $H_{c2}(T)$, which is the scaling field for this theory.

In the case of high-temperature superconductors the irreversibility field H^* has been usually adopted as the scaling field. Nevertheless, some authors[38] argued that the simple substitution of H_{c2} by H^* is without theoretical justification because thermal activation is not taken into consideration. An analysis of the scaling law of the volume pinning force in presence of thermally activated flux motion has been performed by Niel[38] making evident that in a general case there is no clear separation between the field and temperature dependences and hence, that no scaling of $F_P(B,T)$ should be observed in all the cases in presence of flux creep.

In our case, a very good scaling of the pinning forces is obtained using H^* as the scaling field in a very large range of temperatures and fields (see Fig. 11), while the scaling is completely destroyed when H_{c2} is used instead of H^* and this is an experimental fact also reported by other authors.[39,40] We have found that a quadratic relationship exists between $H^*(T)$ and $F_{P\ max}(T)$ (see Fig. 12) and that the field at which $F_P(T)$ reaches its maximum, $H_{F_{p\ max}}(T)$, coincides with the starting point for the field region where we have observed the law $J_c \propto H^{-3}$ to hold, i.e., $H_{F_{p\ max}}(T)$ is the

FIG. 10. Log-log plot of J_c^{ab} vs H showing the existence of a region with H^{-3} dependence of J_c^{ab} above the $H_{F_{p\ max}}$ corresponding to the large bundle regime.
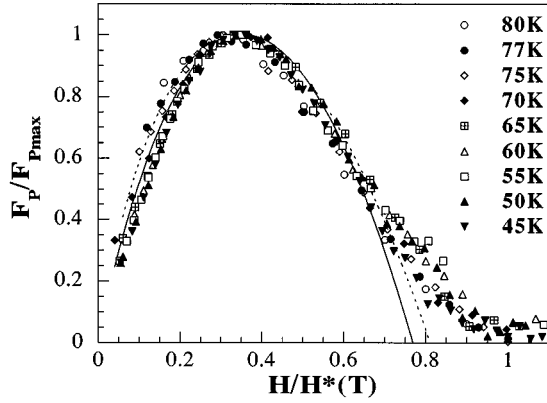
FIG. 11. Reduced volume pinning force vs reduced magnetic field using $H^*(T)$ as scaling field for the sample with 28% of 211 phase and 1% of CeO_2. The solid line corresponds to the fitting by using Eq. (9) and the dashed by using Eq. (8) in the text.

crossover line of the H-T phase diagram between the small bundle regime and the large bundle regime that extends up to the irreversibility line.

Notice that the low-field region where the law $J_c \approx H^{-\alpha}$ with $\alpha \approx 0.3$–0.5 has been observed, is not included in the scaling curve depicted in Fig. 11 because they do not collapse in a single curve. It is clear then that scaling only occurs in the small and large bundle regimes which is actually a consequence of the fact that the same pinning potentials dominate the behavior of $J_c(H,T)$ and $H^*(T)$ in these regimes.

Single flux-creep-based models of the scaling phenomena have been presented recently to analyze $Bi_2Sr_2CaCu_2O_8$ crystals[41,42] and $YBa_2Cu_3O_7$ thin films.[43] In these models the Anderson-Kim relationship [Eq. (1)] is assumed and different field dependences for the effective activation energy U_0, are examined. Following this approach and imposing our experimental observation that $F_{P\ max} \propto H^{*2}$ we get

$$F_P \propto H^{*2}h[1-(\beta h)^{2/3}], \qquad (8)$$

where $\beta = H^*/H_0$, being $H_0 = \alpha(T)/[KT \ln(\tau/\tau_0)]$ and $h = H/H^*$, provide $U(H) = \alpha(T)/H$ as observed in
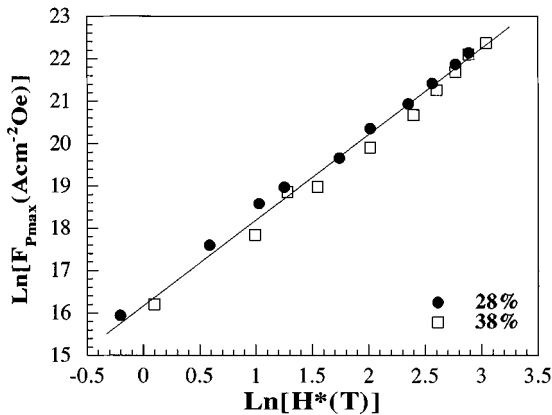

FIG. 12. Relationship between H^* and $F_{P\ max}$ for two of the samples having different content of 211 phase.
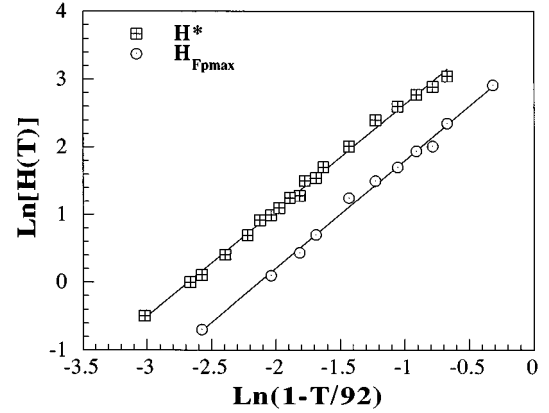
$YBa_2Cu_3O_7$ thin films.[43] However, studies in melt-textured ceramics[44,45] suggest that $U_0 = \alpha(T)/H^{1/2}$ and hence

$$F_P \propto H^{*2}h[1-\beta^{2/3}h^{1/3}], \qquad (9)$$

where $\beta = H^*/H_0^{1/2}$.

The fit of the experimental data obtained using the scaling functions given by Eqs. (8) and (9) are shown in Fig. 11. Neither gives a complete proper description of the experimental data since the complex field dependence of the critical currents is not included in Eqs. (8) and (9). In the small bundle regime we have observed that $J_c(H)$ is essentially constant ($\alpha \approx 0.1$) thus leading to an approximate law $F_P \propto h$ below the maximum $F_{P\ max}$, which is indeed included in Eqs. (8) and (9) as a low-field limit. Above this maximum in the large bundle regime, the observed field dependence $J_c \propto H^{-3}$ is not included as a limiting law in either Eq. (8) or Eq. (9), and hence the fitting falls when approaching the irreversibility line. Nevertheless, the fact that a good scaling is observed in such a large region of temperature and fields makes evident that the pinning mechanisms are the same in this wide region, and since it is observed for different samples whatever this mechanism is, it should be present in all the samples.

3. Irreversibility line

The irreversibility line of our samples has been determined from the point where persistent currents, determined from zero-field-cooled and field-cooled (ZFC-FC) temperature-dependent curves, vanish. For fields above 5.5 up to 22 T, the IL has been determined from isothermal hysteresis loops. In Fig. 13 we show the IL for the sample having 38% of 211 precipitates with the field applied parallel to the c axis together with the field where the macroscopic pinning force reaches its maximum value $H_{F_{p\ max}}(T)$. It is worth mentioning here that there is no correlation between the tiny variations observed in the IL of different samples and their actual content on the 211 phase. These tiny variations may be attributed to small differences with respect to the optimum oxygenation of the samples.[29] The temperature dependence of the IL is properly described by using the following expression:

FIG. 13. Irreversibility line with $H\|c$, and $H_{F_{p\ max}}$ for the sample with 38% of 211 phase and 1% CeO_2. The dashed line correspond to the fitting by using Eq. (10) in the text.

$$H^*(T) = H_0[1 - T/T_c]^m \qquad (10)$$

with $m \approx 3/2$, and no change to a more pronounced temperature dependence down to $T/T_c \approx 0.5$ has been detected. A crossover in the power-law behavior of the IL was observed in electron-doped superconductors[46] and in hole-doped superconductors including oxygen-deficient $YBa_2Cu_3O_{7-\delta}$ and $Bi_2Sr_2CaCu_2O_8$.[47] Some controversy exists regarding the fundamental origin of this crossover phenomenon and whether it is an intrinsic property common to all cuprates superconductors, or a material-dependent effect linked to the particular structure of the pinning centers, is a difficult question to answer. Almasan *et al.*[48] suggested that the crossover is an scale-invariant universal characteristic of the high-T_c superconductors, independent of the superconducting copper-oxide material, the value of T_c and the experimental procedure used to measure $H^*(T)$ and that the crossover temperature is $T/T_c \approx 0.6$. As our data clearly show (see Fig. 13) we have not found signals of the change of the m exponent of Eq. (10) down to $T/T_c \approx 0.5$. Even more, we have observed that $H(F_{P\,max})$, i.e., the field at which the pinning force reaches its maximum value, has the very same temperature dependence that $H^*(T)$ (see Fig. 13) and it does not show any change down to $T/T_c \approx 0.25$. These results clearly indicate that the crossover from $m = 3/2$ to a different value observed in some high-temperature superconductors is not a universal behavior and it should be related to the anisotropy of the system or to extrinsic properties such as the structure of the pinning centers. In the framework of the flux-creep model, the value of the exponent m is determined by the physics of the pinning potential and a change in the value of m would imply the existence of two different regimes in which the pinning potential displays different temperature and/or magnetic-field dependences. Of course, these different temperature and/or magnetic-field dependences would also imply the destruction of the scaling of the pinning forces when data coming from both regimes are put together. The fact that a very good scaling is observed by using data from 85 to 40 K ($T/T_c \approx 0.45$), that are clearly below the proposed universal crossover temperature $T/T_c \approx 0.6$, gives strong clues of the extrinsic origin of such a crossover on the temperature dependence of the IL.

IV. DISCUSSION

Among all the different possible pinning centers existing in our 211/123 directionally solidified samples we have gained strong evidence, from the analysis of the field and temperature dependence of the critical currents, that 211 inclusions do have an important contribution to the irreversible magnetization, in agreement with previous investigations.[4,9,19] This observation, however, has raised a fundamental question about the nature of the pinning mechanism and whether the 123/211 interface itself or the structural defects associated with it are actually the active pinning centers.[4,25] It has already been demonstrated by TEM investigations[19,25] that sharp 123/211 interfaces at the atomic scale are obtained if the oxygenation process is not excessive,[29] thus supporting the assessment that these interfaces have indeed an effective role as pinning centers.

It is also clear by now that the magnetic phase diagram of the 123/211 textured composites is quite complex because
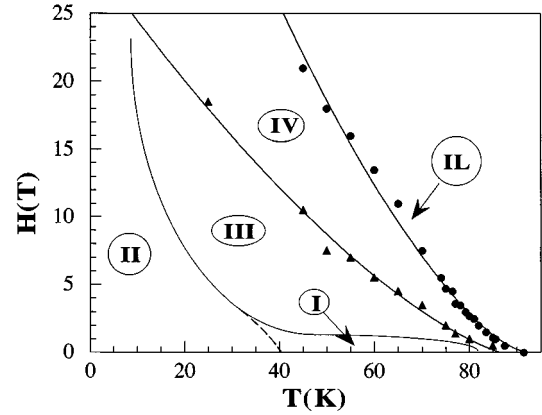

FIG. 14. Magnetic phase diagram of the mixed state of the 211/123 composites obtained by using the sample having 38% of 211 phase and 1% of CeO_2. Region I: Correlated disorder single vortex pinning. Region II: Single vortex with several pinning centers. Region III: Small bundle regime. Region IV: Large bundle regime. See the text for details.

different behaviors have been identified in different regions of field and temperature. Of course the main source of complexity in these materials is the microstructure itself because several types of point, line, and planar defects coexist. The pinning energies associated to these defects will strongly differ and so we must expect that thermal activation will smear the efficiency of a given defect at a certain temperature. It may happen then that the observed behavior does not match any single idealized theoretical prediction in all the temperature ranges but only in a restricted region. This means that a detailed analysis of the different regions of the H-T phase diagram is needed to assess the relative relevance of all the different pinning mechanisms in the observed irreversible magnetic behavior of these samples.

At this point it will be useful to recall all the different regions of the H-T diagram identified through the analysis of the experimental data presented above. First we will summarize the main features of each region together with the experimental facts that allow their identification. A detailed discussion of the pinning mechanism in each of them and a comparison with results obtained in related materials will be presented later.

From the $J_c(T)$ data in the low-field regime we have shown that for temperatures above 40 K, $J_c(T)$ is well described by Eq. (5) displaying the behavior expected for linear correlated disorder.[23] This is the so-called region I in the H-T phase diagram given in Fig. 14 corresponding to a sample having 38% of 211 phase and $V/d = 3450$ cm^{-1}. We have also shown that in this region pinning is clearly dominated by single vortex pinning mechanism at the 123/211 interfaces with a field dependence $J_c \propto H^{-1/2}$. Increasing the field in this high-temperature regime, $J_c(H)$ curves exhibit a region of weak-field dependence labeled as region III. The crossover from the low field $J_c \propto H^{-1/2}$ dependence to a weaker dependence occurs at about $1-1.5$ T. We have argued that pinning in this region could be understood as due to small bundles. Further increasing the field, a region where $J_c(H) \propto H^{-3}$ is reached. This region, labeled as region IV in Fig. 14, has been associated with large bundles of vortices and is upper bounded by the IL.

Going back to the low-field regime, on lowering the temperature below 40 K the footprints associated with single vortex pinning by 123-211 interfaces are smeared out. In this region, labeled as region II, $J_c(T)$ may still be described by a single vortexlike dependence but the linear correlation between $J_c(T)$ and V/d is not well established due to the progressive contribution of other defects with weaker pinning strength.

After this brief description of the magnetic phase diagram we will proceed to a more detailed discussion of the different regions. In region I the vortices are flexible enough to bend and pin at the sharp interfaces with 211 precipitates. Several similarities of this behavior can be drawn with that predicted and observed for systems with columnar pins where the core becomes also nonsuperconducting.[49,50] First, at low enough fields all the vortices will pin at the interfaces of the 211 particles crossing the vortex core while at higher fields some kind of matching field will also exist. Now, however, we should not expect a pure Bose glass phase any more because several vortices will be able to become pinned at the same precipitate. The crossover field now will probably correspond to the saturation of the 211-123 interfaces as pinning centers and this is not simply related to the mean separation between the precipitates. Actually the field where a crossover is observed in Fig. 14 corresponds to $H \approx 1$ T and the FLL spacing is $a_f = 450$ Å which is about ten times smaller than the mean separation between particles. If we assume that in this single vortex regime all the vortices of a normally undistorted FLL crossing a 211 particle become pinned at the interface, the observed crossover field ($H \approx 1$ T) corresponds to a mean separation of about 20 Å between the vortices located at the interface, which is very near to the coherence length ξ_{ab} of YBa$_2$Cu$_3$O$_7$ and thus the minimum distance between neighboring vortices.

The precipitate size is much less than the dimensions of the samples thus meaning that vortices will consist, in this temperature region, of short pieces having virtually infinite tilt modulus c_{44}, similarly to the Bose glass phase, separated by interstitial vortex fragments thermally depinned from weaker pinning centers. Overall, the fraction of vortex length pinned at the 211 interfaces will be roughly proportional to $V^{1/3}$. The crossover field will mark then a turnover in the flux dynamics because above this field (region III) the small bundles will be formed which will also correlate with these interstitial regions with weaker pinning centers.

As we have mentioned before in connection with the observed temperature dependence of the critical currents, we obtained a much better linearity with the V/d parameter from the constants fitted in region I, i.e., the law expected from correlated disorder defects. This is still a further clue giving support to our conclusion that the enhancement of J_c arises from 211 interfaces because the nonrelaxed pinning force increases (J_c^0 increases linearly with V/d) and the thermal activation decreases (T^* increases linearly with V/d).

On the other hand, we would like to point out that the net increase of critical currents with the V/d parameter clearly signals the right direction for improvement of the superconducting characteristics of the 123/211 composites. Further reduction of the size of 211 particles, as performed with Pt (Ref. 51) or CeO$_2$ (Ref. 28) additions, allows us to increase steadily the critical currents and it is conceivable that

through improvement of the processing methodology the present values of critical currents ($J_c^{ab} = 10^5$ A/cm^2) can be raised by an order of magnitude approaching those observed in thin films at 77 K ($J_c^{ab} = 10^6$ A/cm^2).

On lowering the temperature below $T = 40$ K a progressive departure from the laws expected from a simple correlated disorder pinning occurs. First the power-law dependence of the critical currents still holds but the exponent becomes progressively smaller down to $\alpha = 0.3$ at 5 K. The region where this occurs is indicated as II in the phase diagram (Fig. 14). In this region the temperature dependence of J_c has evolved to a new behavior consistent with single vortex pinning as predicted by collective-pinning theory for weak pinning centers. The observed upraise of $J_c(T)$ in this region is enhanced when the V/d parameters increases, as clearly evidenced by the higher slope of the straight line associated with J_{00} as compared to that of J_c^0 in Fig. 3(a). The meaning of this observation is that there is some coupling between the concentration of secondary defects originating in the low-temperature vortex glass behavior and the 123-211 interface. Then, we could speculate about the existence of a second-order effect concerning the interface-induced generation of defects which also contribute to pin the vortices at low temperature. We note also that the crossover temperature from region I to region II is very similar to the thermal depinning temperature observed in single crystals, indicating in that case the crossover from single vortex regime to small bundle regime.[52] It is very likely then that below this temperature the vortex fragments occupying interstitial regions between 211 particles become pinned by local defects, which should be very similar to those existing in single crystals. This phenomenon should also be reflected in the dynamic behavior of the vortices and this is presently under investigation.

We note that the potential law observed in the low-temperature single vortex pinning regime ($J_c \approx H^{-0.3}$) is exactly the same observed in thin films recently investigated by Griessen et al.,[24] where it was concluded that pinning was dominated by mean-free-path fluctuations (δl pinning). It might happen then that similar weak pinning centers superpose to strong pinning by interfaces leading to the same potential law for J_c. In single crystals at 5 K, a quasi-field-independent behavior starts at much lower fields,[52] then the strong pinning by 211-123 interfaces appears to be responsible for the up displacement of the borderline between regions II and III observed in textured composites. Actually, upon decreasing the temperature the definition of this line becomes progressively difficult because in the small bundle regime the field dependence of J_c is slightly increased when decreasing temperature thus approaching the same law of the single vortex regime.

Instead, the line marking the crossover from region I to III, i.e., from single vortex to small bundle regimes at high temperatures, is easier to detect. The identification of this intermediate-field region as a small bundle regime has been recently carried out by Thompson et al. in YBa$_2$Cu$_3$O$_7$ single crystals.[16] This temperature range corresponds actually to that where usually fishtail anomalies are detected in YBa$_2$Cu$_3$O$_7$.[53] Our work suggests that these anomalies originate in the small bundle regime when the effects of interface pinning is moderate or null as in single crystals.[52] The single

vortex pinning regime observed in region I does not exist in single crystals because the thermal activation makes ineffective the weak pinning centers but when the cooperative effects of the flux-line lattice increase at high fields J_c might be enhanced thus leading to fishtail anomalies. In 123/211 composites this situation does not occur because a single vortex regime persists at such high temperatures and hence the low-field critical currents are higher and the fishtail anomalies are decreased or eliminated. If the critical currents in the small bundle regime are enhanced by means of proton or ion irradiation,[16,17] for instance, these effects are also washed out.

Finally, we should briefly discuss the main features of the so-called region IV in the general phase diagram. In this region the field dependence of J_c is characteristic of the large bundle regime. The onset of this regime is found to be marked approximately by the maximum of the pinning force and, as it should be expected, preliminary relaxation measurements suggest that in this region there is a sudden enhancement of the flux-creep effects. We have demonstrated that despite the relevance of the flux-creep effects, a good scaling of the pinning forces may be reached by using solely the irreversibility line. As the maximum pinning force $F_{P_{\max}}$ and the field where this occurs $H_{P_{\max}}$ are related to $H^*(T)$ by simple power laws, the observed scaling reflects the fact that a common thermal depinning phenomena influence these parameters and the critical currents in regions III and IV. We note, however, that the proportionality constants between $H^*(T)$ and these parameters may differ in samples having different concentration of 211 precipitates. This means that even if the irreversibility line appears to be quite independent of the concentration of 211 precipitates the critical currents may be still somehow enhanced in the small and large bundle regimes, as it has been observed by other authors in melt-textured 211/123 composites.[45] From a practical point of view our work indicates that measurements performed at 77 K are not very useful to establish a correlation between microstructure and pinning mechanisms in 123/211 composites because the crossover between regions I, III, and IV occur very closely. We suggest that inductive measurements at lower temperatures, for instance $T=60$ K, may be much more useful because the interface single vortex pinning regime can be easily separated from the small bundle regime where interstitial defects also have a non-negligible role.

V. SUMMARY AND CONCLUSIONS

We have investigated the field and temperature dependence of the critical currents in the $H\|c$ configuration of textured $YBa_2Cu_3O_7$-Y_2BaCuO_5 composites having different concentration of nonsuperconducting 211 precipitates. From this wide investigation and a good knowledge of the microstructure of the ceramic composites we have been able to propose a magnetic phase diagram H-T where several regions corresponding to different pinning regimes are identified. The first and more outstanding characteristic of this system is the existence of randomly distributed precipitates which can pin vortices at the sharp interfaces. These defects can be classified as a source of correlated disorder lying parallel to the vortices in any field orientation and thus it is a

strong pinning center which will influence the critical currents and the flux dynamics.

A single vortex pinning regime with 211/123 interfaces as dominating pinning centers has been unambiguously identified. The region where this is the dominating pinning mechanism is indicated as I in the H-T phase diagram (Fig. 14). However, due to the relatively large separation between the 211 precipitates a crossover field must exist in concomitance with a saturation effect of the interface pinning mechanism. This behavior is very similar to the matching field, or equivalent dose field B_ϕ, in crystals with columnar defects. When this crossover field is overcome the vortices will start to pin at other, weaker, pinning centers existing between these precipitates. In this new situation the interaction energy between the vortices become comparable to the pinning energy and thus we enter in the conditions of the small bundle regime, in the sense defined by the collective-pinning theory. This pinning regime is identified as that characteristic of region III in the phase diagram (Fig. 14). In this region the pinning force is not simply related to any determined pinning center. The critical currents will be influenced in a complex manner by all kind of defects existing in the matrix. This point has been demonstrated by several authors which have shown that the amount of 211 precipitates, the concentration of dislocations and the separation between twin planes have some influence in the critical currents $J_c^{ab}(H)$. We note also that this region is where typically the so-called "fishtail" effects are observed and hence we could speculate that different pinning centers lie at the heart of this anomalous behavior.

On the other hand, we have also identified a low-temperature region extending up to very high fields (beyond 20 T at 5 K). This region is characterized by a power-law dependence of the critical currents $J_c(H) \approx H^{-\alpha}$, with $\alpha \approx 0.3$, and it's interpreted as a single vortex regime with several types of pinning centers being effective simultaneously. The transition between the high-temperature phases, region I (single vortex interfacial pinning) or region III (small bundle regime), and this new low-temperature phase is smooth but it is clearly identified in both the field and the temperature dependences of $J_c(H,T)$. At low temperature and high fields this phase completely wipes out, in our best samples, the small bundle regime. Also the temperature dependence of J_c at low fields can be described in region II by a law typical of a vortex glass with weak point defects while at high temperature we could fit $J_c(T)$ to the law expected for systems with correlated disorder and Bose glass behavior.[23] It is very likely then that the line separating region I and II corresponds to a depinning line for the weaker defects. In this way at low temperature, phase II will correspond to a mix up of the different pinning centers, while phase I is actually very akin to the behavior observed in systems with columnar defects.

Finally, we have shown that a simple relationship exists between the maximum pinning force $F_p^{\max}(T)$ and the irreversibility line $H^*(T)$ and also that pinning forces scale in the regions III and IV of the H-T phase diagram. The actual meaning of the scaling of the pinning forces is that the same pinning centers and thermal activation effects are being effective in different samples in these particular regions of the phase diagram. This is consistent with our observation that $H^*(T)$ is basically independent of the concentration of 211 particles in the sample, i.e., the defects which dominate the vanishing of the pinning force are very similar in all our

123/211 composites. In conclusion, the present work has demonstrated that even if the microstructure of melt-textured 123/211 composites is very complex, firm conclusions concerning the flux-pinning mechanisms may be reached which serve as a very useful guide for the improvement of the superconducting performances of these materials for practical applications.

ACKNOWLEDGMENTS

[1] D. Dimos, P. Chaudhari, J. Mannhart, and F. K. LeGoues, Phys. Rev. Lett. **61**, 219 (1988).

[2] J. W. Ekin, A. I. Braginski, A. J. Panson, M. A. Janocko, D. W. Capone, N. J. Zuluzec, B. Flandermeyer, O. F. De Lima, M. Hong, J. Kwo, and S. H. Liou, J. Appl. Phys. **62**, 4821 (1987).

[3] S. Jin, T. H. Tiefel, R. C. Sherwood, R. V. van Dover, M. E. Davis, G. W. Kammlott, and R. A. Fastnacht, Phys. Rev. B **37**, 7850 (1989).

[4] K. Salama and D. F. Lee, Supercond. Sci. Technol. **7**, 177 (1994); K. Salama, V. Selvamanickam, and D. F. Lee, in *Processing and Properties of High-T_c Superconductors*, edited by Sungho Jin (World Scientific, Singapore, 1993), Vol. 1, pp. 155–211.

[5] S. Piñol, F. Sandiumenge, V. Gomis, B. Martinez, J. Fontcuberta, X. Obradors, E. Snoeck, and C. Roucau, in *Applied Superconductivity*, edited by H. C. Freyhardt (DGM-I-Verlag, Oberursel, 1993), p. 365; S. Piñol, V. Gomis, B. Martínez, A. Labarta, J. Fontcuberta, and X. Obradors, J. Alloys Compounds **195**, 11 (1993).

[6] P. W. Anderson and Y. B. Kim, Rev. Mod. Phys. **36**, 39 (1964).

[7] D. S. Fisher, M. P. A. Fisher, and D. A. Huse, Phys. Rev. B **43**, 130 (1991); M. P. A. Fisher, Phys. Rev. Lett. **62**, 1415 (1989).

[8] M. V. Feigel'man, V. B. Geshkenbein, and V. M. Vinokur, Phys. Rev. B **43**, 6263 (1991); M. V. Feigel'man and V. M. Vinokur, *ibid*. **41**, 8986 (1990).

[9] H. Fujimoto, T. Taguchi, M. Murakami, N. Nakamura, and N. Koshizuka, Cryogenics **32**, 954 (1992).

[10] W. K. Kwok, U. Welp, G. W. Crabtree, K. G. Vandervoort, R. Hulscher, and J. Z. Liu, Phys. Rev. Lett. **64**, 966 (1990).

[11] V. Selvamanickam, V. Mironova, S. Son, and K. Salama, Physica C **208**, 238 (1993); V. Selvamanickam, V. Mironova, and K. Salama, J. Mater. Res. **8**, 249 (1993).

[12] V. M. Pan, V. L. Strechnikov, V. F. Solovjov, V. F. Taborov, H. W. Zandbergen, and J. G. Won, Supercond. Sci. Technol. **5**, 707 (1992).

[13] Z. L. Wang, A. Goyal, and D. M. Kroeger, Phys. Rev. B **47**, 5373 (1993).

[14] B. Martínez, V. Gomis, S. Piñol, I. Catalan, J. Fontcuberta, and X. Obradors, Appl. Phys. Lett. **63**, 3081 (1993); B. Martínez, S. Piñol, V. Gomis, F. Sandiumenge, N. Vilalta, J. Fontcuberta, and X. Obradors, IEEE Trans. Appl. Supercond. **5**, 1611 (1995).

[15] M. Murakami, S. Gotoh, H. Fujimoto, K. Yamaguchi, N. Koshizuka, and S. Tanaka, Supercond. Sci. Technol. **4**, S43 (1991).

[16] J. R. Thompson, Yang Ren Sun, D. K. Christen, L. Civale, A. D. Marwick, and F. Holtzberg, Phys. Rev. B **49**, 13 287 (1994).

[17] L. Civale, A. D. Marwick, T. K. Worthington, M. A. Kirk, J. R. Thompson, L. Krusin-Elbaum, Y. Sun, J. R. Clem, and F. Holtzberg, Phys. Rev. Lett. **67**, 648 (1991).

[18] F. M. Sauerzopf, H. P. Wiesinger, W. Kristcha, H. W. Weber, M. C. Frischherz, and H. Gerstemberg, Cryogenics **33**, 8 (1993).

[19] M. Murakami, K. Yamaguchi, H. Fujimoto, N. Nakamura, T. Taguchi, N. Koshizuka, and S. Tanaka, Cryogenics **32**, 930 (1992); *Melt Processed High-Temperature Superconductors*, edited by M. Murakami (World Scientific, Singapore, 1992), p. 192.

[20] M. Murakami, H. Fujimoto, S. Gotoh, K. Yamaguchi, N. Koshizuka, and S. Tanaka, Physica C **185-189**, 321 (1991).

[21] B. Martínez, V. Gomis, S. Piñol, J. Fontcuberta, and X. Obradors, Physica C **235-240**, 3007 (1994).

[22] V. V. Moshchalkov, V. V. Metlushko, G. Güntherodt, I. N. Goncharov, A. Yu. Didyk, and Y. Bruynseraede, Phys. Rev. B **50**, 639 (1994).

[23] D. R. Nelson and V. M. Vinokur, Phys. Rev. Lett. **68**, 2398 (1992); Phys. Rev. B **48**, 13 060 (1993).

[24] R. Griessen, Wen Hai-hu, A. J. J. Van Dalen, B. Dam, J. Rector, H. G. Schnack, S. Libbrecht, E. Osquiguil, and Y. Bruynseraede, Phys. Rev. Lett. **72**, 1912 (1994); Wen Hai-hu, H. G. Schnack, R. Griessen, B. Dam, and J. Rector, Physica C **241**, 353 (1995).

[25] F. Sandiumenge, S. Piñol, X. Obradors, E. Snoeck, and C. Roucau, Phys. Rev. B **50**, 7032 (1994).

[26] E. M. Gyorgy, R. B. van Dover, K. A. Jackson, L. F. Schneemeyer, and J. V. Waszczak, Appl. Phys. Lett. **55**, 283 (1989); H. P. Wiesinger, F. M. Sauerzopf, and H. W. Weber, Physica C **203**, 121 (1992).

[27] S. Piñol, F. Sandiumenge, B. Martínez, N. Vilalta, X. Granados, V. Gomis, F. Galante, J. Fontcuberta, and X. Obradors, IEEE Trans. Appl. Supercond. **5**, 1549 (1995).

[28] S. Piñol, F. Sandiumenge, B. Martínez, V. Gomis, J. Fontcuberta, and X. Obradors, Appl. Phys. Lett. **65**, 1448 (1994).

[29] B. Martínez, F. Sandiumenge, S. Piñol, N. Vilalta, J. Fontcuberta, and X. Obradors, Appl. Phys. Lett. **66**, 772 (1995); F. Sandiumenge, N. Vilalta, S. Piñol, B. Martinez, and X. Obradors, Phys. Rev. B **51**, 6645 (1995).

[30] V. Gomis, S. Piñol, B. Martínez, J. Fontcuberta, and X. Obradors, in *Applied Superconductivity*, edited by H. C. Freyhardt (DGM-I-Verlag, Oberursel, 1993), p. 373.

[31] M. R. Beasley, R. Labusch, and W. W. Webb, Phys. Rev. **181**, 682 (1969).

[32] E. Zeldov, N. M. Amer, G. Koren, A. Gupta, M. V. McElfresh, and R. J. Gambino, Appl. Phys. Lett. **56**, 680 (1990).

[33] J. R. Thompson, Yang Ren Sun, L. Civale, A. P. Malozemoff, M. W. McElfresh, A. D. Marwick, and F. Holtzberg, Phys. Rev. B **47**, 14 440 (1993).

[34] L. Krusin-Elbaum, L. Civale, V. M. Vinokur, and F. Holtzberg, Phys. Rev. Lett. **69**, 2280 (1992).

[35] W. A. Fietz and W. W. Webb, Phys. Rev. **178**, 657 (1969).

[36] A. M. Campbell and J. E. Evetts, Adv. Phys. **21**, 199 (1972); D.

Dew-Hughes, Philos. Mag. **30**, 293 (1974).

[37] E. J. Kramer, J. Appl. Phys. **44**, 1360 (1974).

[38] L. Niel, Cryogenics **32**, 975 (1992).

[39] K. Kishimoto, Y. Nakayoma, N. Motohira, T. Noda, T. Kobayashi, K. Kitazawa, K. Yamafuji, I. Tamaka, and H. Kojima, Supercond. Sci. Technol. **5**, 68 (1992).

[40] R. Wördenweber, K. Heizemann, G. V. S. Sastry, and H. C. Freyhardt, Cryogenics **29**, 458 (1990).

[41] H. Yamasaki, K. Endo, S. Kosaka, M. Umeda, S. Yoshida, and K. Kajimura, Phys. Rev. Lett. **70**, 3331 (1993).

[42] J. T. Kucera, T. P. Orlando, G. Virshup, and J. N. Eckstein, Phys. Rev. B **46**, 11 004 (1992).

[43] J. D. Hettinger, A. G. Swanson, W. J. Skocpol, J. S. Brooks, J. M. Graybeal, P. M. Mankiewich, R. E. Howard, B. L. Straughn, and E. G. Burkhardt, Phys. Rev. Lett. **62**, 2044 (1989); S. Zhu, J. R. Thompson, E. C. Jones, R. Feenstra, D. H. Lowndes, and D. P. Norton, Phys. Rev. B **46**, 5576 (1992).

[44] F. Galante, J. Fontcuberta, and X. Obradors (private communication).

[45] P. J. Kung, M. P. Maley, M. E. McHenry, J. O. Willis, M. Murakami, and S. Tanaka, Phys. Rev. B **48**, 13 922 (1993).

[46] Y. Dalichaouch *et al.*, Phys. Rev. Lett. **64**, 599 (1990); C. C. Almasan, C. L. Seaman, Y. Dalichaouch, and M. B. Maple, Physica C **174**, 93 (1991).

[47] J. T. Seidler, T. F. Rosenbaum, D. H. Heinz, J. W. Downey, A. P. Paulikas, and B. W. Veal, Physica C **183**, 333 (1991); K. Kadowaki and T. Mochiku, *ibid.* **195**, 127 (1992).

[48] C. C. Almasan, M. C. de Andrade, Y. Dalichaouch, J. J. Neumeier, C. L. Seaman, M. B. Maple, R. P. Guertin, M. V. Kuric, and J. C. Garland, Phys. Rev. Lett. **69**, 3812 (1992).

[49] L. Krusin-Elbaum, L. Civale, and C. Feild, Physica C **235-240**, 2801 (1994).

[50] G. Blatter, M. V. Feigel'man, V. B. Geshkenbein, A. I. Larkin, and M. V. Vinokur, Rev. Mod. Phys. **66**, 1125 (1994).

[51] N. Ogawa, I. Hirabayashi, and S. Tanaka, Physica C **177**, 101 (1991).

[52] L. Krusin-Elbaum, L. Civale, V. M. Vinokur, and F. Holtzberg, Phys. Rev. Lett. **15**, 2280 (1992).

[53] V. Gomis, I. Catalan, F. Perez, B. Martinez, J. Fontcuberta, A. Fuertes, and X. Obradors, Cryogenics **33**, 39 (1993).